Covalent Bonding and Charge Density in Diamond*

L. KLEINMAN†
Institute for the Study of Metals, University of Chicago, Chicago, Illinois

AND

J. C. PHILLIPS
Department of Physics and Institute for the Study of Metals, University of Chicago, Chicago, Illinois

(Received July 17, 1961; revised manuscript received September 11, 1961)

Recently Göttlicher and Wölfel have measured x-ray scattering factors from diamond powder that differ appreciably from the older values of Brill. Because scattering from the 1*s* core is small, information about the crystal covalent band can be obtained. In the Brillouin zone theory of crystal wave functions the valence charge density varies throughout the valence band. Free-atom approximations to the diamond charge density replace the sp^3 crystal wave functions at $\mathbf{k}=0$ by atomic sp^3 charge densities. This approximation is insufficient to explain covalent bonding effects, such as the "forbidden" reflection F_{222}. We have examined crystal charge densities *throughout* the valence band. We find that there are two important mechanisms which affect the valence charge density. The first is a linear response to the ionic potentials. This may be called dielectric screening; it is dominant in metals, and it gives no contribution to F_{222}. The second is nonlinear in the ionic potentials, and may be called crystal hybridization; it is responsible for covalent effects in the charge density, and it makes no contribution to F_{220}. The contributions of both mechanisms to F_{111}, F_{220}, F_{222}, F_{311}, and F_{400} have been computed. Surprisingly, the results are in good agreement with the older data of Brill and simple models of the covalent bond, while significant disagreement with Göttlicher and Wölfel's measurements is found.

1. INTRODUCTION

FOR some time it has been customary to calculate x-ray scattering factors in crystals from a superposition of free-atom charge densities. The latter are obtained from either Hartree or Hartree-Fock solutions of the Schrödinger equation for free atom configurations which are supposed to be good approximations to the states actually present in the crystal.

This procedure is open to two objections. Even though the crystal potential may be given accurately by a superposition of atomic potentials, crystal wave functions must satisfy periodic boundary conditions. As a result, the atomic energy levels are broadened into energy bands. Because of the translational periodicity of the lattice, the crystal energy levels can be labeled by Bloch wave vectors $\mathbf{k}$ in the Brillouin zone.[1] For example, the valence bands of diamond are shown in Fig. 1 for two principal symmetry axes of the Brillouin zone.

Another objection is that the crystal potential should be determined not from *ad hoc* assumptions but from a self-consistent solution of the Schrödinger equation. In this way the departure of the crystal charge density from a superposition of atomic charge densities is treated including the effect of overlapping atomic potentials which modify the valence contribution to the crystal potential.

For most experiments these corrections are too small to be measurable. For example, asphericities in *d*-electron charge distributions in transition metals could not be measured by x rays,[2] but some small asphericities may have been detected by using polarized neutrons.[3] The latter measure the charge distribution of unpaired spins, so that the large core background which obscured the x-ray results was absent.

Another favorable case is that of diamond. Here the core is very small and because of the strong covalent bond asphericities are large. Many attempts have been made, both experimentally and theoretically, to examine the covalent bond in diamond. Göttlicher and Wölfel[4] have recently made a painstaking study of x-ray scattering from diamond powder. We compare our results with experiment in Sec. 3.

Recently we have carried out calculations of the wave functions in diamond at a number of points in the valence band.[5] The valence charge density, defined as a suitably weighted average over the band, was

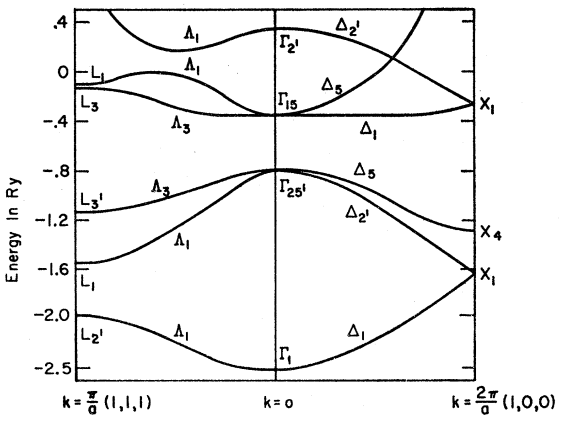

FIG. 1. Sketch of the energy bands of diamond along [100] and [111] axes of the Brillouin zone. The twofold degenerate states at the top of the valence band (Δ_5 and Λ_3) contribute strongly to the covalent bonding.

* Supported in part by Office of Naval Research.

† Present address; Department of Physics, University of Pennsylvania, Philadelphia 4, Pennsylvania.

[1] H. Jones, Proc. Roy. Soc. (London) **A144**, 225 (1934).

[2] B. W. Batterman, D. R. Chipman, and J. J. Demarco, Phys. Rev. **122**, 68 (1961).

[3] R. Nathans and A. Paoletti, Phys. Rev. Letters **2**, 252 (1959).

[4] S. Göttlicher and E. Wölfel, Z. Elektrochem **63**, 891 (1959).

[5] L. Kleinman and J. C. Phillips, Phys. Rev. **116**, 880 (1959), hereafter called I.

expanded in the Fourier series

$$\rho_v(\mathbf{r})=\sum_{\mathbf{K}} F_{v\mathbf{K}}e^{i\mathbf{K}\cdot\mathbf{r}}, \tag{1.1}$$

where $\mathbf{K}$ is a reciprocal lattice vector, and $F_{v\mathbf{K}}$ is the usual x-ray scattering factor for the valence charge density. From an examination of the crystal potential we concluded that only $F_{v\mathbf{K}_1}$, $\mathbf{K}_1=2\pi a^{-1}(\pm1, \pm1, \pm1)$, would be large enough to make an important contribution to the crystal potential. The charge density was treated self-consistently with regard to $F_{v\mathbf{K}_1}$, while the other $F_{v\mathbf{K}}$'s were given their free-atom values.

Because the higher Fourier coefficients of the valence potential are small relative to the corresponding Fourier coefficients of the core potential, this approximation is sufficiently accurate for setting up the orthogonalized plane wave (OPW) matrix elements. However, comparison with precision x-ray data requires a detailed examination of the other $F_{v\mathbf{K}}\sim K^2V_{v\mathbf{K}}$. A striking example is the "forbidden" reflection F_{222}. This is zero in the free-atom approximation because the structure factor vanishes. Renninger's nonzero value[6,7] is a direct measure of covalent bonding in the crystal. Comparable corrections are expected for F_{220}, F_{311}, and F_{400}.

A qualitative description of the important physical conclusions to be drawn from our somewhat involved calculations is given in Sec. 2. A detailed technical description of our methods, which we hope will be of use to others making self-consistent studies of crystal charge densities, is given in the Appendix.

2. CRYSTAL WAVE FUNCTIONS

Because the crystal charge density is given quite well to a first approximation by a superposition of atomic charge densities it seems natural to make the tight-binding approximation and expand the crystal Bloch function as a superposition of atomic wave functions,

$$\psi_{\mathbf{k}}(\mathbf{r})=\sum_{vl} e^{i\mathbf{k}\cdot\mathbf{R}_v}\phi_l(\mathbf{r}-\mathbf{R}_v), \tag{2.1}$$

where l denotes carbon wave functions ($2s$, $2p$, $3s$, etc.). Because wave functions from different atoms overlap, this basis set can describe asphericities in the charge density due to covalent bonding. One can also augment the atomic basis set with, e.g., Gaussian functions centered midway between two atoms. In this way Ewald and Hönl[8,9] hoped to obtain a simple description of the effect of covalent bonding including only overlap of nearest neighbors. Later experience has shown, however, that overlap between more distant neighbors must be included, e.g., in graphite to fifth neighbors.[10]

We have therefore used a different basis set, that of orthogonalized plane waves (OPW's).[5] This basis set has the advantage that almost all the charge density is automatically obtained in the Fourier form (1.1). The charge density associated with a plane wave is constant. We showed[5] that the interference between different plane waves added constructively throughout the valence band to produce a value of F_{111} in good agreement with experiment. The same interference is expected to be much smaller for other reciprocal lattice vectors, as we shall now see.

Let us assume that the effect of orthogonalization can be included in the crystal potential

$$V(\mathbf{r})=\textstyle\sum_{\mathbf{K}} V_{\mathbf{K}}e^{i\mathbf{K}\cdot\mathbf{r}}, \tag{2.2}$$

in the way discussed by Cohen and Phillips[11] and used by us in I. Then if our unperturbed wave functions are plane waves, first-order perturbation gives

$$\psi_{\mathbf{k}}=\psi_{\mathbf{k}}^{(0)}+\sum_{\mathbf{K}}\frac{\langle\mathbf{k}+\mathbf{K}|V_{\mathbf{K}}|\mathbf{k}\rangle}{E_{\mathbf{k}}-E_{\mathbf{k}+\mathbf{K}}}\psi_{\mathbf{k}+\mathbf{K}}^{(0)}, \tag{2.3}$$

$$\psi_{\mathbf{k}}^{(0)}=e^{i\mathbf{k}\cdot\mathbf{r}}, \quad \psi_{\mathbf{k}+\mathbf{K}}^{(0)}=e^{i(\mathbf{k}+\mathbf{K})\cdot\mathbf{r}}. \tag{2.4}$$

The linear treatment of crystal fields implied by (2.2)–(2.4) leads to a dielectric screening picture of crystal charge densities when it is carried out self-consistently.[11] This procedure is justified whenever the crystal potential V is sufficiently weak.

There are two objections to this procedure in diamond. As we have pointed out in I, $V_{\mathbf{K}_1}$ is much larger than $V_{\mathbf{K}_n}$, $\mathbf{K}_n\neq\mathbf{K}_1$. This means that the effect of $V_{\mathbf{K}_1}$ in second order may be as large or larger than $V_{\mathbf{K}_n}$ in first order. In particular second-order effects of V_{111} make almost all the contributions to F_{222}.

The second objection is that (2.3) is based on nondegenerate perturbation theory. The orbitals of p atomic symmetry oriented transverse to the crystal momentum $\hbar\mathbf{k}$ are exactly degenerate along the [100] and [111] directions in Fig. 1. They remain quasi-degenerate (in the sense that their energy separation is small compared to $V_{\mathbf{K}_1}$) throughout the Brillouin zone. Consequently these bands tend to hydridize strongly, with $\rho_{\mathbf{K}_n}$ admixed into $\rho_{\mathbf{K}_1}$ in such a way as to increase charge density along the bonding directions where the attractive potential is largest.

Some insight into the hybridization of crystal wave functions can be obtained by considering the expansion

$$\psi_{\mathbf{k}}=e^{i\mathbf{k}\cdot\mathbf{r}}\textstyle\sum_{\mathbf{K}} C_{\mathbf{k}}^{\mathbf{K}}e^{i\mathbf{K}\cdot\mathbf{r}}. \tag{2.5}$$

If we first approximate $\psi_{\mathbf{k}}$ by $e^{i\mathbf{k}\cdot\mathbf{r}}$, then the $C_{\mathbf{k}}^{\mathbf{K}}$ that are strongly effected by hybridization are those associated with $\mathbf{K}=\mathbf{K}_1$. Because $k\leq K_F$ this means (see Fig. 2) that the volume of momentum space $k'\leq K_F+K_1$ must be treated exactly, allowing for nonlinear terms in V_{K_1} and interference of V_{K_1} with V_{K_n}. For $k'\geq K_F+K_1$ only V_{K_n} are involved, and as

[6] M. Renninger, Z, Krist. **97**, 107 (1937).
[7] M. Renninger, Acta Cryst. **8**, 606 (1955).
[8] P. P. Ewald and H. Hönl, Ann. Physik **25**, 281 (1936).
[9] P. P. Ewald and H. Hönl, Ann. Physik **26**, 673 (1936).
[10] F. J. Corbato, Ph.D. thesis, Massachusetts Institute of Technology, 1956 (unpublished).
[11] M. H. Cohen and J. C. Phillips, Phys. Rev. **124**, 1818 (1961).

these are small they can be treated by the linear approximation (2.3). Figuratively speaking, linear dielectric screening is valid for $k' \geq K_F + K_1$, that is, outside the hybridization volume.

Within the hybridization volume the Schrödinger equation must be solved at a number of points in the valence band large enough to give a good sample. Because of the quasi-degeneracy of the transverse-p valence band, the techniques we have invoked to make our sampling are quite involved, and they are described in the Appendix.

We conclude with some qualitative remarks about hybridization. Following Ewald and Hönl, Brill[12] has represented the charge density as a superposition of atomic charges plus a bonding charge centered between nearest neighbors. The scattering factors are then

$$\begin{aligned} F_{111} &= f_C/\sqrt{2} + f_\epsilon, \\ F_{220} &= f_C, \\ F_{311} &= f_C/\sqrt{2} - f_\epsilon, \\ F_{222} &= -2f_\epsilon, \\ F_{400} &= f_C - 2f_\epsilon, \end{aligned} \tag{2.6}$$

where $f_C(K)$ is the form factor for the spherically symmetric charge densities located on the carbon sites and $f_\epsilon(K)$ the form factor for the bonding charge. The *signs* of the bonding contributions in (2.6) should be compared with our F_{bond} as given in Table IV. It will be seen that qualitatively the charge within the hybridization volume conforms quite closely to the f_ϵ of the Ewald-Hönl-Brill model. Also f_C represents the scattering from the 1s electrons and the "dielectric screening" part of the valence charge density. However, it is difficult to determine $f_\epsilon(K)$ quantitatively from Table IV and (2.6). Thus we see no simple way to define the "number of electrons" in the covalent bond.

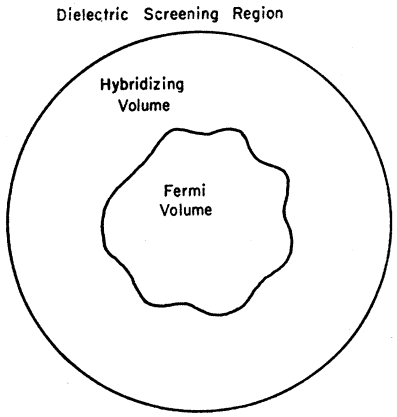

FIG. 2. All k space is divided in three parts. The Fermi volume is that part of k space which is occupied in the limit of weak crystal potential. Those states which are mixed into states in the Fermi volume by V_{111} constitute the hybridizing volume. The rest of k space is available to react to the higher and weaker V_K and forms the dielectric screening region.

[12] R. Brill, Z. Elektrochem. **63**, 1088 (1959).

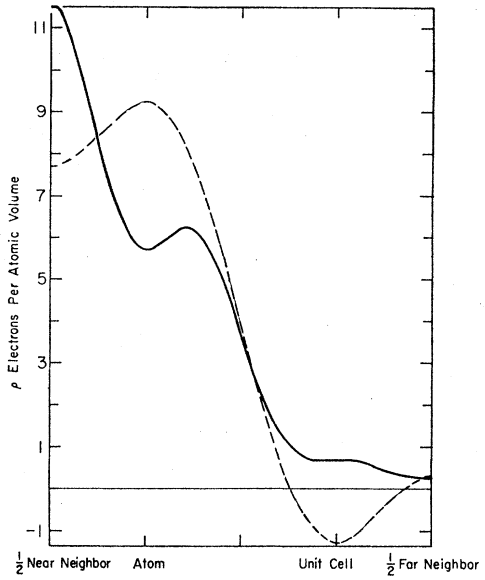

FIG. 3. Valence charge density along a [111] axis in diamond. The dashed line is the charge density obtained from $F(0)$ and F_{111} alone. The solid line is obtained from $F(0)$, F_{111}, F_{220}, F_{311}, F_{222}, and F_{400} computed from the hybridizing region of k space only. The orthogonalization to the 1s core function has not been included. Note the effect of hybridization is to transfer charge from the atom to the covalent bond.

Alternatively we may plot the crystal charge density along a [111] direction connecting nearest neighbors (Fig. 3). Notice that all F_{K_n} add constructively between the atoms to give a sizeable amplification of the bonding charge due to F_{111} alone.

3. COMPARISON WITH EXPERIMENT

The experimental results of Göttlicher and Wölfel[4] are listed in Table I together with the older results of Brill *et al.*[13] Göttlicher and Wölfel measured integrated intensities for powder samples while Brill measured F_{K_1} and F_{K_n} for a single crystal and then corrected for extinction by comparing with a powder measurement of F_{K_1}. Göttlicher and Wölfel also compared the experimental and theoretical scattering factors for larger K (where the 1s electrons alone contribute to the scattering). They thereby determined a Debye-Waller correction $\exp(MK^2)$ with M in good agreement with the Debye temperature of diamond (2200°K). The corrected scattering factors are given in columns 4 and 5. Scattering factors for the 1s electrons[14] are listed in column 6, and when these are subtracted from the experimental values one obtains the experimental valence scattering factors (columns 7 and 8).

In Table II we compare the two sets of experimental valence scattering factors with theoretical ones from superposition of Hartree-Fock atomic charge densities[14]

[13] R. Brill, H. G. Grimm, C. Herman, and C. Peters, Ann. Physik **34**, 393 (1939).

[14] D. T. Keating and G. H. Vineyard, Acta Cryst. **8**, 606 (1955).

TABLE I. Absolute values of x-ray scattering factors. Values measured by Brill *et al.* (column 2) and by Göttlicher and Wölfel (column 3) are listed in units of electrons per atom. Columns 4 and 5 list these results multiplied by an appropriate Debye-Waller factor. Column 6 lists the 1*s* Hartree-Fock core contributions to the scattering factors which when subtracted from columns 4 and 5 gives the experimental valence contributions to the scattering factors.

K	BGHP	GW	Corrected BGHP	Corrected GW	1*s*	Val. BGHP	Val. GW
111	2.33	2.32	2.35	2.34	1.36	0.99	0.98
220	1.81	1.91	1.86	1.97	1.79	0.07	0.18
311	1.06	1.13	1.11	1.18	1.22	−0.11	−0.04
222		0.14[a]		0.15[a]	0		±0.15[a]
400	1.38	1.39	1.47	1.48	1.62	−0.15	−0.14

[a] Measured by Renninger (references 6 and 7).

(column 3), Ewald and Hönl's tight-binding values, and our values. Note that our values consist of a hybridization part and a dielectric screening part, and that the former makes a negligible contribution to F_{220}, and the latter a negligible contribution to F_{222} (Table IV in the Appendix).

From Table II we see that for F_{222} our results improve considerably on those of Ewald and Hönl, and are in substantial quantitative agreement with Renninger's experimental value. Because F_{222} is a direct measure of asphericities in the charge distribution about each atom, our results represent the first successful attempt to calculate bonding asphericities using Bloch band functions.

In view of our success with respect to F_{222}, we should expect our estimates of the bonding corrections to other scattering factors also to be satisfactory. In the case of F_{220} in particular our calculations give a very small valence contribution, in agreement with the bonding model (2.6). The experimental results of Göttlicher and Wölfel disagree significantly (by about 10% in F_{220}) with this conclusion. Because of the great care taken by Göttlicher and Wölfel to eliminate systematic errors, this 10% discrepancy warrants further discussion.

There are three possible sources of error in our Hartree-Fock calculation:

1. The crystal potential may be inaccurate.
2. The calculated charge density may be inaccurate because too few plane waves were used in the expansion of ψ_k.
3. The sampling of the valence band may be too coarse, because only 32 states in the extended zone were treated.

TABLE II. Comparison of valence contribution to scattering factors. Columns 2 and 3 are the experimental values from Table I. Column 4 is a superposition of free-atom Hartree-Fock charge densities. Column 5 is the tight-binding calculation of Ewald and Hönl and column 6 the present plane-wave calculation.

K	Val. BGHP	Val. GW	Free atom	Tight binding	Plane wave
111	0.99	0.98	0.84	0.80	0.88
220	0.07	0.18	0.19		0.01
311	−0.11	−0.04	0.03		−0.14
222		±0.15	0	−0.03	−0.15
400	−0.15	−0.14	−0.03		−0.13

The errors coming from the first two sources are easily seen to be quite small. Changes in the crystal potential cause small changes in the charge density, because the core potential is fixed and is much larger than the uncertain parts of the electronic potential. (For example, in I a Hartree potential gave practically the same value for F_{111} as a Hartree-Fock potential.) Similarly our "dielectric" corrections should be accurate to 30%, and they give the corrections to ψ_k that would be obtained from a complete set of plane waves.

It is difficult to put an upper limit on the errors coming from 3. Our experience with studying wave functions away from symmetry points in the Brillouin zone gives us considerable confidence in our results, especially with the "$\mathbf{k}\cdot\mathbf{p}$" corrections discussed in the Appendix. These appear to be the largest error in the sampling procedure, and even these terms are more than 3 times too small to explain the discrepancies with experimental results.

The self-consistent procedures used here have been programmed for very high speed computers by several workers.[15] A check on our results with these programs appears to be worthwhile, because theoretical confirmation of our calculated charge densities would call into question the accuracy of modern powder x-ray techniques.

We are grateful to Dr. H. C. Bolton for bringing this problem to our attention.

APPENDIX

We describe here in some detail the sampling of valence-band charge densities. As we indicated in Sec. 2, the quasi-degeneracy of bands complicates the sampling considerably. The degeneracy is greatest at the symmetry points where we have calculated charge densities, so that we tend to overestimate hybridization effects. We describe here methods used to correct for this tendency.

[15] F. Herman (private communication) and F. Quelle (private communication).

TABLE III. Contribution of valence bands computed to 65 plane waves to scattering factors. The singular terms which result from interference of a particular symmetrized combination of plane waves (SCPW) with itself are listed in parenthesis next to the regular terms which result from interference between different SCPW. In computing the total contribution to any F, each term must be multiplied by the degeneracy and weighting factors listed in columns 2 and 3.

Term	D	W	F_{111}	F_{220}	F_{311}	F_{222}	F_{400}
Γ_1	1	1	0.0218	0.0002 (0.0020)	−0.0014	−0.0011 (−0.0010)	−0.0015
$\Gamma_{25'}$	3	1	0.0401	0.0078 (−0.0064)	−0.0091	−0.0060 (−0.0062)	−0.0033 (−0.0048)
X_1	2	3	0.0285	0.0003 (0.0019)	−0.0017	−0.0025	−0.0006
X_4	2	3	0.0277	0.0059 (−0.0088)	−0.0058	−0.0004 (−0.0036)	−0.0022 (−0.0043)
L_1	1	4	0.0230 (−0.0099)	−0.0040 (0.0027)	0.0009 (0.0008)	−0.0001	−0.0013
$L_{2'}$	1	4	0.0172 (0.0139)	0.0041 (0.0009)	−0.0023 (−0.0001)	−0.0021	−0.0017
$L_{3'}$	2	4	0.0197 (0.0138)	0.0080 (−0.0099)	−0.0045 (−0.0057)	−0.0074	−0.0059
Total			0.924	0.002	−0.160	−0.145	−0.127

The charge density is sampled at 32 points of high symmetry in the extended reciprocal lattice. The sampling procedure has been described in detail in I in connection with the calculation of F_{111}. In the case of F_{111} each subzone contributes approximately equally, as one would conclude from first-order perturbation theory [Eq. (2.3)]. For the higher F's, because of hybridization this is no longer the case. We have therefore divided the contribution from each point into regular and singular terms. By singular term we mean the following. Crystal symmetry requires that basis functions consist not of single orthogonalized plane waves but of certain symmetrized combinations of orthogonalized plane waves. A simple example is the first basis function at $\mathbf{L}=\pi a^{-1}(1,1,1)$, which is

$$|\alpha_1\rangle=(1/\sqrt{2})[\exp(i\mathbf{L}\cdot\mathbf{r})+\exp(-i\mathbf{L}\cdot\mathbf{r})]. \quad (2.7)$$

Now in the calculation of $\rho=\psi^*\psi$ interference between different plane waves in $|\alpha\rangle$ will contribute oscillatory terms to the charge density which are essentially independent of the sign of V_{111}. For instance, $|\alpha_1\rangle$ as described by (2.7), will contribute to F_{111}.

In Table III the singular and regular contributions to the various F's are listed. It can be seen that a large contribution to F_{222} comes from the threefold degenerate state at $\mathbf{k}=0$ of p atomic symmetry, $\Gamma_{25'}$. It would be incorrect to treat this term by the sampling procedure used for the regular terms which are more nearly constant over the zone, since the "accidental" symmetry of $|\alpha_1\rangle_{25'}$ is rapidly lost as one goes away from $\mathbf{k}=0$ in the valence band. Instead $\psi_\mathbf{k}$ is expanded in terms of ψ_0 by the usual $\mathbf{k}\cdot\mathbf{p}$ perturbation theory[16] for $\mathbf{k}$ near 0, and an exact analysis of the secular equation is carried out for larger values of $\mathbf{k}$ when $\mathbf{k}$ lies along certain symmetry directions. The sum over the Brillouin zone can then be done approximately in the neighborhood of $\mathbf{k}=0$. The result for the subzone about Γ is 0.65 ± 0.15 times the value which the sampling procedure would have given. A similar calculation shows that no correction is necessary for the singular contribution to F_{222} from X_4. Thus the listed singular terms have each been multiplied by an appropriate factor less than 1. This complication in calculating the singular contribution is not intrinsic and would be overcome with a finer sampling of k space. These results which were computed from the plane-wave part of the OPW's are listed in the first row of Table IV. The additional contributions obtained when plane waves are orthogonalized to the $1s$ core are listed in the second row of Table IV. We choose to list the two contributions separately because although both terms contribute to the x-ray scattering, only the plane-wave part contributes to the covalent bond (see Fig. 3).

These charge densities were obtained from wave functions calculated in I from an expansion of 65 OPW. This includes all the hybridizing volume of k space (see Fig. 2). In order to test the convergence of our solutions we carried our calculations to more tahn 400 OPW for state $\Gamma_{25'}$ (p electrons at $k=0$). Beyond 65 OPW the s electrons contribute practically nothing to the charge density. Hence we are able in row 3 of Table IV to list an estimate of the additional contributions to the scattering factors beyond 65 OPW. At $k=0$ there are three p states and one s state, compared to two and two throughout most of the valence band, so that row 3 should be an overestimate.

This estimate can also be made by computing the dielectric screening directly. It was shown by Cohen and Phillips[11] that

$$V_{\text{eff}}^{\mathbf{K}}=V_{\text{ion eff}}^{\mathbf{K}}+V_s^{\mathbf{K}}=V_{\text{ion eff}}^{\mathbf{K}}/\epsilon(K,0), \quad (A1)$$

where $V_{\text{ion eff}}^{\mathbf{K}}$ is the $\mathbf{K}$th Fourier component of the effective ionic potential, $V_s^{\mathbf{K}}$ the screening potential and $\epsilon(K,0)$ the static dielectric constant given by

$$\epsilon(K,0)=1-\frac{4\pi e^2}{K^2}\sum_{\mathbf{k}}\frac{N_\mathbf{k}-N_{\mathbf{k}+\mathbf{K}}}{E_\mathbf{k}-E_{\mathbf{k}+\mathbf{K}}}, \quad (A2)$$

where N is the occupation number of the unperturbed states. Using Poisson's equation, we obtain the screening charge density

$$F_{\mathbf{K}}{}^s=\frac{\Omega K^2}{8\pi}\frac{1-\epsilon(K,0)}{\epsilon(K,0)}V_{\text{ion eff}}^{\mathbf{K}}, \quad (A3)$$

where Ω is the atomic volume. Because we are interested

[16] G. Dresselhaus, A. F. Kip, and C. Kittel, Phys. Rev. **98**, 556 (1955).

TABLE IV. Bonding and dielectric screening contributions to x-ray scattering factors. Rows 1 and 3 are quantities listed in Tables III and V and row 2 is the contribution of the oscillatory part of the valence wave function to the scattering factors: row 5 is their total. Row 3 lists the additional contributions to the various scattering factors beyond those obtained from an expansion of 65 plane waves. The Brillouin zone was sampled only at $k=0$ for these additional contributions.

	F_{111}	F_{220}	F_{311}	F_{222}	F_{400}
65 plane waves	0.924±0.08	0.002±0.04	−0.160±0.04	−0.145±0.04	−0.127±0.04
Orthogonalization terms	−0.041	−0.047	−0.011	−0.002	−0.020
$\Gamma_{25'}$ estimate beyond 65 plane waves	···	0.058	0.039	···	0.030
Dielectric screening beyond 65 plane waves	···	0.047	0.031	···	0.017
Total	0.88	0.01	−0.14	−0.15	−0.13

in large $\mathbf{K}$ for which $E_K \gg E_g$, the energy gap in the semiconductor, we can approximate $\epsilon(K,0)$ by its value for a free electron gas which is well known to be given by

$$\epsilon(K,0)=1+\frac{2K_F}{\pi a_0 K^2}\left[1+\frac{K_F}{K}\left(1-\frac{K^2}{4K_F{}^2}\right)\times\ln\left|\frac{K+2K_F}{K-2K_F}\right|\right], \quad \text{(A4)}$$

where a_0 is the Bohr radius $\hbar^2/me^2$.

Now an electron of wave number $\mathbf{k}$ can have the state $\mathbf{K}+\mathbf{k}$ mixed into it by $V_{\text{ion eff}}{}^{\mathbf{K}}$ only if $|\mathbf{K}+\mathbf{k}|>J$, the radius of the hybridization volume. (If $|\mathbf{K}+\mathbf{k}|<J$ we have already counted its contribution to ϵ in our 65 OPW expansion.) Thus Eq. (A4), which is obtained by integrating over the whole Fermi volume, is valid when hybridization is present only if $K+K_F>J$. If $K-K_F<J<K+K_F$, then the dielectric constant must be obtained in integrating over that part of the Fermi sphere which in Fig. 4 lies outside the sphere J. This is done in the cylindrical coordinates y, ρ, φ shown in Fig. 4 and the result is

$$\epsilon'(K,0)=1+\frac{2}{\pi a_0 K^3}\left[K_F{}^2\ln\left|\frac{2KK_F+K^2}{J^2-K_F{}^2}\right|-J^2\ln\left|\frac{2JK-K^2}{J^2-K_F{}^2}\right|-\frac{K^2}{4}\ln\left|\frac{2K_F+K}{2J-K}\right|+\tfrac{1}{2}(K_F{}^2-J^2+KK_F+KJ)\right]. \quad \text{(A5)}$$

If $K-K_F<J$ then since the entire Fermi sphere lies within J, $\epsilon'(K,0)=0$. Values of $\epsilon(K,0)$ and $\epsilon'(K,0)$ are compared in Table V for the three values of K of interest. J was taken to be $|2\pi a^{-1}(2,2,2)|$ because the $\mathbf{k}$ with the largest magnitude in the jagged Fermi sphere (Fig. 2) is $2\pi a^{-1}(1,1,1)$. $V_{\text{ion eff}}{}^{\mathbf{K}}$, which is also listed in Table V, is taken from Cohen and Phillips.[11] Using $V_{\text{ion eff}}{}^{\mathbf{K}}$, $\epsilon'(K,0)$, and Eq. (A3), we calculate the changes in the charge density obtained due to dielectric screening beyond the covalent bonding region of k space. These are listed in Table V and also Table IV where they are added to the covalent bonding contributions (65 plane wave expansion). They are seen to be relatively small and their effect is to lessen somewhat the peaking of the charge density between nearest neighbors due to hybridization.

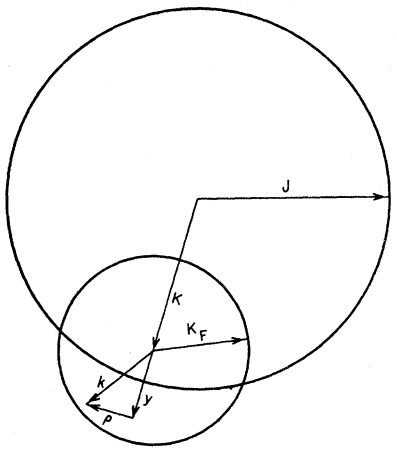

FIG. 4. Region of k space that contributes to dielectric screening of V_k. Fermi volume of Fig. 2 is replaced by sphere centered at end of vector $\mathbf{K}$. If $\mathbf{K}+\mathbf{k}$ lies outside the hybridizing volume (sphere of radius J) then the state $\mathbf{K}+\mathbf{k}$ is mixed into the state $\mathbf{k}$ by V_k. The integration over $\mathbf{k}$ of Eq. (A2) is done in the cylindrical coordinates y, ρ, φ.

TABLE V. Dielectric screening of effective ionic potential. Columns 2 and 3 list $\epsilon(K,0)-1$ as computed for a free electron gas and for a free electron gas in which only those electrons with $\mathbf{k}$ such that $|\mathbf{K}+\mathbf{k}|\geq|2\pi a^{-1}(2,2,2)$ can contribute to ϵ. Column 4 lists the Kth Fourier component of the average effective ionic potential. In column 5 is listed $F_{\mathbf{K}}{}^s$, the screening charge responding to $V_{\text{ion eff}}{}^{\mathbf{K}}$ due to ϵ' of column 3.

$\mathbf{K}$	$\epsilon-1$	$\epsilon'-1$	$V_{\text{ion eff}}{}^{\mathbf{K}}$	$F_{\mathbf{K}}{}^s$
$2\pi a^{-1}(2,2,2)$	0.173	0.023	−0.20	0.047
$2\pi a^{-1}(3,1,1)$	0.076	0.024	−0.09	0.031
$2\pi a^{-1}(4,0,0)$	0.030	0.021	−0.04	0.017